The Optical Gravitational Lensing Experiment. Search for Planetary and Low-Luminosity Object Transits in the Galactic Disk. Results of 2001 Campaign*

A. Udalski[1], **B. Paczyński**[2], **K. Żebruń**[1], **M. Szymański**[1], **M. Kubiak**[1], **I. Soszyński**[1], **O. Szewczyk**[1], **Ł. Wyrzykowski**[1], **and G. Pietrzyński**[3,1]

[1]Warsaw University Observatory, Al. Ujazdowskie 4, 00-478 Warszawa, Poland
e-mail:
(udalski,zebrun,msz,mk,soszynsk,szewczyk,wyrzykow,pietrzyn)@astrouw.edu.pl
[2] Princeton University Observatory, Princeton, NJ 08544-1001, USA
e-mail: bp@astro.princeton.edu
[3] Universidad de Concepción, Departamento de Fisica, Casilla 160–C, Concepción, Chile

ABSTRACT

We present results of an extensive photometric search for planetary and low-luminosity object transits in the Galactic disk stars commencing the third phase of the Optical Gravitational Lensing Experiment – OGLE-III. Photometric observations of three fields in the direction of the Galactic center (800 epochs per field) were collected on 32 nights during time interval of 45 days. Out of the total of 5 million stars monitored, about 52 000 Galactic disk stars with photometry better than 1.5% were analyzed for flat-bottomed eclipses with the depth smaller than 0.08 mag.

Altogether 46 stars with transiting low-luminosity objects were detected. For 42 of them multiple transits were observed, a total of 185, allowing orbital period determination. Transits in two objects: OGLE-TR-40 and OGLE-TR-10, with the radii ratio of about 0.14 and estimate of the radius of the companion $1.0 - 1.5$ $R_{\rm Jup}$, resemble the well known planetary transit in HD 209458.

The transiting objects may be Jupiters, brown dwarfs, or M dwarfs. Future determination of the amplitude of radial velocity changes will establish their masses, and will confirm or refute the reality of the so called "brown dwarf desert". The low mass stellar companions will provide new data needed for the poorly known mass-radius relation for the lower main sequence.

All photometric data are available to the astronomical community from the OGLE Internet archive.

1. Introduction

In the past decade astronomers witnessed a breathtaking progress in the search for extrasolar planets. The discovery of mysterious planet-like objects around pulsar PSR B1257+12 (Wolszczan and Frail 1992) was followed by the detection

*Based on observations obtained with the 1.3 m Warsaw telescope at the Las Campanas Observatory of the Carnegie Institution of Washington.

of the first solar type planets around nearby stars (Mayor and Queloz 1995, Marcy and Butler 1996). While the former type system seems to be unique and its origin and status remain mysterious, the solar type planets seem to be quite common in the solar neighborhood: up to now about 80 planetary systems have been reported (see *http://exoplanets.org* for the most recent information).

Apart from PSR B1257+12, whose discovery was based on radio wavelength pulse time delay measurements, ultra-precise measurements of the radial velocity shifts in the optical spectra of target stars were the main successful method of planet detection. Such measurements provided orbital periods and minimum masses of the companion (*cf.* Mazeh and Zucker 2002, and references therein).

Extensive spectroscopic searches of nearby dwarf stars revealed a large variety of planetary orbits. A distinct class is a group of several stars with Jupiter-mass planets orbiting their stars in several days (a<0.1 a.u.), and called "51 Peg-like" planets or "hot Jupiters". A very important feature of this class is a relatively large probability that a planetary orbit has an inclination allowing a transit in front of the star. While for our solar system such a probability would be very small (Sackett 1999), it is about 10% for "51 Peg-like" planets. The expected depth of a transit is small, $\approx$1% even for "Jupiters". However, this is within reach of a careful ground-based photometry.

It is not surprising that the "51 Peg-like" planets were monitored photometrically. At the end of 1999 a spectacular discovery of the first transit of a planet around HD 209458 was announced by Henry *et al.* (2000) and Charbonneau *et al.* (2000). Combined spectroscopic data and photometry of the transit allow to determine the most important planet parameters, its mass and radius: 0.7 $M_{\rm Jup}$ and 1.4 $R_{\rm Jup}$, respectively, for HD209458 (Brown *et al.* 2001).

The discovery of HD 209458 transit proved that photometry may be used in search for planets. However, due to a small probability of transits, a photometric survey must monitor a large number of stars with high photometric accuracy every $\approx$10 minutes for many nights. The most promising areas of the sky are the dense stellar regions like the Galactic disk, globular clusters etc. Ground-based accurate photometry used to be difficult in crowded fields. It has recently become possible thanks to the technique called "image subtraction" or "difference image analysis" (DIA) developed by Alard and Lupton (1998) and Alard (2000).

Several planetary transit monitoring programs are presently underway. Gilliland *et al.* (2000) monitored 47 Tuc globular cluster with the HST telescope. No transit was found in 34 000 stars monitored over the period of 8.3 days. The same cluster was also monitored from the ground (Sackett 2000, private communication). Other programs are focused on open clusters fields (Quirrenbach *et al.* 2000, Street *et al.* 2000, Mochejska *et al.* 2002), Galactic disk fields (Mallen-Ornelas, Seager and Yee 2002, private communication), or brighter stars – STARE project (Brown and Charbonneau 2000). Also space missions for continuous photometric monitoring of nearby stars, capable to detect Earth-like planet transits, like COROT (Deleuil *et al.* 2000) and KEPLER (*http://www.kepler.arc.nasa.gov*) are planned. However, HD 209458 remains the only planetary transit system known.

The photometry alone cannot unambiguously distinguish between Jupiter size planets and other low-luminosity objects: brown dwarfs and late type M dwarfs, as all of them have the radii of the order of 0.1–0.2 $R_\odot$ (1–2 R_{Jup}). Thus, a spectroscopic follow-up and a measurement of the radial velocity amplitude of the stars is needed to determine the masses of transiting companions.

Although detection of planets *via* transits is certainly the most exciting possibility, detection of any other type of low-luminosity objects is also very important. There appears to exist so called "brown dwarf desert": absence of brown dwarfs with short period orbits around stars (*cf.* Tabachnik and Tremaine 2001, and references therein). The mass-radius relation for the lower main sequence is poorly known, and a serious discrepancy between the observations and models can be seen (Torres and Ribas 2001, O'Brien, Bond and Sion 2001, *cf.* Spruit 1982, Spruit and Weiss 1986, for a possible explanation). Summarizing, photometric detection of transits, combined with the spectroscopic follow-up, will provide valuable information about all three types of low luminosity stellar companions.

The Optical Gravitational Lensing Experiment (OGLE) is a long term observational program started almost a decade ago (Udalski *et al.* 1992, Udalski, Kubiak and Szymański 1997) with the initial goal of detection of microlensing events *via* photometric monitoring of millions of stars in the densest stellar regions of the sky. The OGLE survey turned out to be very successful in discovering not only hundreds of microlensing events (Udalski *et al.* 1993, Woźniak *et al.* 2001) but also providing huge amount of data on the variable (Udalski *et al.* 1999, Żebruń *et al.* 2001, Woźniak *et al.* 2002) and non-variable (Udalski *et al.* 1998, Udalski *et al.* 2000) stars in the Galactic bulge and Magellanic Clouds and contributing to many other fields.

At the beginning of 2001, the OGLE project underwent its second major hardware upgrade. A single chip 2048×2048 pixel CCD camera was replaced by the second generation eight chip 8192×8192 pixel CCD mosaic. Also the old data reduction pipeline was replaced with the new one based on image subtraction. The data flow of the survey increased by almost an order of magnitude, and the accuracy of photometry reached the millimagnitude level for the brightest stars.

The third phase of the OGLE survey, OGLE-III, started on June 12, 2001. For the first 45 days three fields located in the densest stellar regions in the direction of the Galactic center were monitored continuously up to 35 times per night, on a total of 32 nights, for detection of short time-scale stellar variability. These data are ideal to search for planetary transits; this was one of the goals of the campaign. Such a pilot search was undertaken to answer the question whether planetary transit detection is possible and the program is worth continuing in the next observing seasons.

In this paper we present results of the OGLE-III search for planetary and low-luminosity object transits in the photometric data collected during the 2001 campaign. We discovered 185 individual transit cases in 46 objects from about 52 000 Galactic disk stars for which the photometric accuracy was 1.5% or better. These transits may be due to "Jupiters", brown dwarfs or M dwarfs.

The distinction will be possible when a spectroscopic follow-up will be done. The photometry of all OGLE-III stars with transits is available to the astronomical community from the OGLE Internet archive.

2. Observational Data

Observations presented in this paper started the third phase of the OGLE experiment, OGLE-III. They were collected with the 1.3-m Warsaw telescope at the Las Campanas Observatory, Chile, (operated by the Carnegie Institution of Washington) equipped with the new large field CCD mosaic camera, consisting of eight 2048×4096 pixel SITe ST002A detectors. More detailed description of the OGLE-III instrumental system will be presented in the forthcoming paper. Here, we only highlight the most important features of the OGLE-III second generation camera and data reduction system.

The pixel size of each of the detectors is 15 μm giving the 0.26 arcsec/pixel scale at the focus of the Warsaw telescope. The full field of view of the camera is about 35×35.5 arcmins. The reading of the entire array takes about 98 seconds and the size of single full frame is about 137 MB. The gain of each chip is adjusted to be about 1.3 e^-/ADU with the readout noise from about 6 to 9 e^-, depending on the chip. The well depth of chips reaches from 60000 e^- to 80000 e^-. Contrary to the OGLE-II instrumentation, where the vast majority of images were taken in the "driftscan" mode, the new camera only works in the classical "still-frame" mode.

The vast majority of photometric data were taken during 32 nights spanning 45 days from June 12, 2001. After that period single observations of presented fields were done once every few nights till the end of 2001 Galactic bulge season in October 2001. Equatorial coordinates (J2000.0) of the observed fields are listed in Table 1. Each of the fields overlaps slightly with the neighboring one for calibration purposes.

Table 1

Equatorial coordinates of the planetary transit fields

Field	RA (J2000)	DEC (J2000)
BLG100	$17^h51^m00^s$	$-29°59'45''$
BLG101	$17^h53^m40^s$	$-29°49'50''$
BLG102	$17^h56^m20^s$	$-29°30'50''$

Almost all observations were made in the *I*-band filter. The exposure time of each image was set to 120 seconds. Altogether about 800 epochs were collected for each field during the 2001 season. Additionally, several *V*-band frames were also made to have color information for the observed objects. *V*-band images were exposed for 150 seconds.

Because of extremely high stellar density of the observed fields the observations were carried out only during good seeing conditions and were suspended when the seeing exceeded 1.8 arcsec. The median seeing of the presented dataset is 1.2 arcsec.

3. Data Reduction

Similarly to the previous phases of the OGLE survey, data reduction in OGLE-III is supposed to be performed at the telescope in almost real time. However, during the 2001 campaign only the first part of the data reduction pipeline, namely the initial reduction like de-biasing and flat-fielding, was implemented. Photometric reductions of collected images were performed off-line, however, with the same pipeline which will be implemented on-line at the OGLE telescope in 2002 observing season.

The initial reduction procedures were based on the IRAF† CCDRED package routines and were performed automatically when the new frame arrived from the telescope. To make data handling easier, each chip of the mosaic was treated separately. Flat-fielded data, were compressed with the RICE algorithm and stored on a few hundred GB partition of the hard disk, and finally dumped to the HP Ultrium tape (about 200 GB of raw data per tape).

The photometric data reduction was based on the difference image analysis (DIA) method (Alard and Lupton 1998, Alard 2000). The core of the system – image subtraction procedures were based on the implementation of this method by Woźniak (2000), with many software modifications for better performance and stability. Contrary to the Woźniak (2000) approach (which in principle works off-line, well after all images of the field are collected, while presented data pipeline is designed to analyze photometry on-the-fly) photometry on the subtracted image is performed for all objects identified earlier in the reference image at the position of their centroids. Subtracted image is also analyzed for stars which apparently changed their brightness above the preassigned threshold, so that the on-line information on the current variability is obtained. Objects which cannot be cross-identified with reference image stars on the subtracted image are treated as new objects in the current frame (although this list may contain artifacts like small traces of non-perfectly removed cosmic-rays etc.). The threshold for detection of the current variability is by definition too high for triggering by very small amplitude variations like transits. However, full photometric information on the brightness of all objects in the image is preserved in the file with the photometry of all objects.

Next, these files are used to feed the final photometric databases. We use the same database software as during the previous stages of the OGLE project (Szymański and Udalski 1993) with minor modifications due to somewhat different data input format. Separate databases are created for each chip in a

†IRAF is distributed by National Optical Observatories, which is operated by the Association of Universities for Research in Astronomy, Inc., under cooperative agreement with National Science Foundation.

given field, thus the complete set for a field consists of eight databases of about 1 GB each in the case of the Galactic bulge data collected in 2001 season.

The main advantage of the DIA photometry over the classical PSF approach is a much higher accuracy. This is achieved due to two main reasons. First, variability is measured very precisely on an almost empty subtracted image. Secondly, a much better quality profile photometry for constant part of the flux can be obtained from the reference image which has much higher S/N than a single frame, as it is obtained by stacking several (more than 10 in our case) single images. A large number of stars in the observed fields assures a very good match between the reduced and reference images before the subtraction is done.

Woźniak (2000) noted a significantly better quality of photometry obtained with the DIA over the standard OGLE-II data reduction pipeline based on profile photometry. The comparison of the DIA results for OGLE-III frames indicates that the quality of OGLE-III data is even superior over the DIA OGLE-II photometry. This is certainly due to a better sampling (0.26 *vs.* 0.42 arcsec/pixel) and better quality of images obtained in the "still-frame" mode. For the brightest stars *rms* of photometric measurements from all, more than 800, epochs is at a few millimagnitudes level.

Observations in the 2001 season were focused on a detection of rapid variability, and no calibration images with standard stars were collected. Therefore it was not possible to tie directly the photometry to the standard system with a very high precision. However, to have a crude estimate of the zero point of our photometry we compared our instrumental magnitude scale with the well calibrated photometry of OGLE-II fields (Udalski *et al.* 2002, in preparation). In many cases OGLE-II and OGLE-III fields overlap, hence a comparison was possible. If the object was observed during the OGLE-II phase we shifted OGLE-III magnitudes to fit OGLE-II calibrated values. In this case the zero point accuracy is better than 0.05 mag. If there was no OGLE-II/OGLE-III overlap then an average shift resulting from a comparison of other stars in the same field was applied. We believe that the zero point accuracy of our magnitude scale is about 0.1 mag in this case. It should be noted that although OGLE-II photometric measurements exist for large number of our transit objects, they are not suitable for search or even confirmation of transits because of much smaller number of observations, non-appropriate sampling (one observation per 1–3 days) and much worse photometric quality.

Astrometric solution for the observed fields was performed in identical manner as in the OGLE-II photometric maps case (Udalski *et al.* 1998), *i.e.*, by cross-identification of about 2000 brightest stars in each chip image with the Digitized Sky Survey images of the same part of the sky. Then the transformation between OGLE-III pixel grid and equatorial coordinates of the DSS (GSC) astrometric system was calculated. The systematic error of the latter can be up to about 0.7 arcsec, while the internal error of the transformation is about 0.2 arcsec.

4. Selection of Transit Candidates

A huge number of the observed stars requires a fully automatic method of selection of transit candidates for the work to be effective. We performed our search for transits as follows. The three observed fields contain more than 5 million stars, located both in the Galactic disk and in the Galactic bulge. Therefore, we first limited the sample to the stars located in the disk. To do this we observed our fields several times in the V-band. A preliminary reduction of these images was used to construct the photometric databases, similar to the main I-band databases. Next, we prepared the color-magnitude diagrams (CMDs) of the observed fields. One of such diagrams is presented in Fig. 1.

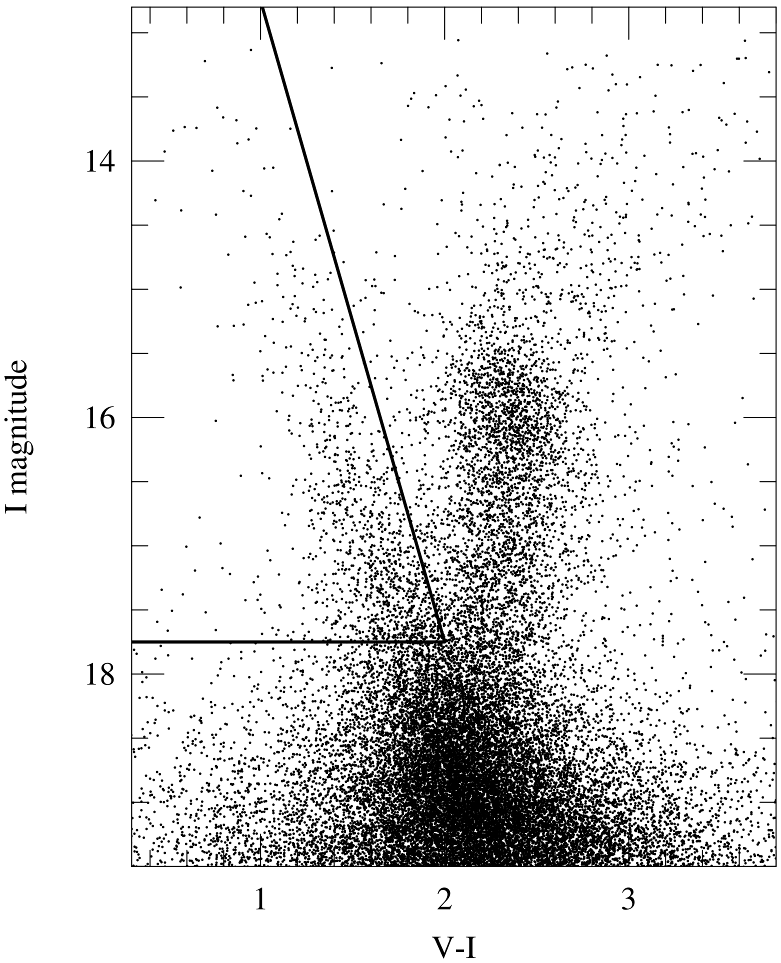

Fig. 1. Color-Magnitude diagram of the BLG102.4 field. Only 20% of stars are plotted for clarity. Solid line limits the Galactic disk stars searched for transits. Accuracy of the zero points of color and I-band magnitude scale is about 0.1 mag.

For brighter stars the separation of the disk main sequence stars (forming a clear sequence in Fig. 1) from the Galactic bulge stars (red giant and subgiant stars) is clear. Hence, further analysis was restricted to the stars from the region limited by bold lines in Fig. 1.

We further limited our sample to the stars with the standard deviation of all observed magnitudes ≤ 0.015 mag. To avoid contamination of the standard deviation by outlying observations we ran 5σ clipping filter on the data prior to the calculations of the standard deviation. We were left with about 52 000 stars in the three fields which passed our initial filtering.

In the next step all these objects were subjected to the transit finding procedure. We constructed an artificial error-less transit light curve with an amplitude of 0.015 mag and the total duration of 0.03 phase. Next, the observations of the analyzed star were folded with a trial period and cross-correlated with the artificial light curve. If the cross-correlation coefficient was larger than a preselected threshold the star was marked as a candidate. The procedure was repeated for trial periods in the range of 1–10 days with a step of $0.0001 \cdot P$.

After the initial tune-up of the cross-correlation coefficient threshold this algorithm worked very effectively. Practically all triggered cases turned out to be small amplitude eclipsing objects and the contamination by artifacts was minimal. The algorithm can easily be used to calibrate the efficiency of our detection procedure by running it on artificially prepared eclipsing light curves. This, however, has not been done yet. The algorithm is very sensitive even to single transit events during our observing run, as there is practically always a period (false, of course) which mimics a regular eclipsing light curve with some gaps in the observations. Such a light curve is easily detected by our search algorithm.

The final selection of candidates was done by careful visual inspection of the photometric data, both in the day scale and phased. We left on the main list of candidates only those stars which have a significant probability of being true transits. We do not present here a large number of small amplitude events caused by grazing eclipses (V-shape eclipses, often with some shift of the secondary eclipse phase) or somewhat deeper (>0.1 mag) cases which occasionally passed our filters. However, one has to remember that a regular faint binary with a flat bottomed eclipse may blend with a much brighter star, to mimic a low amplitude transit. In our very dense stellar fields the probability of blending is non-negligible. Future spectroscopy will resolve this possible problem.

The final periods of our candidates were found by a careful examination of the eclipse light curve, by minimizing dispersion in the eclipse phases. For some objects only uncertain information on periodicity could be found, because only two or so, often incomplete eclipses were registered. When a small number of transits was registered we always adopted the shortest period consistent with our remaining data. The formal accuracy of the period is of the order of $2 \cdot 10^{-4} P$. In a few cases we observed only one transit event so that nothing can be said at this stage about the periodicity of these object.

5. Results of 2001 Campaign

Forty six transit stars were found in the 2001 campaign data among 52 000 searched Galactic disk objects. The star entered the final list of transit objects when the amplitude of transit was smaller than 0.08 mag. With a completely dark transiting object such an amplitude still corresponds to 1.4 $\mathrm{R_{Jup}}$ if the stellar radius is half the solar.

We present the results in the form of a catalog and atlas of light curves. Table 2 contains basic data for each star: abbreviation in the form OGLE-TR-NN, equatorial coordinates (J2000.0 epoch), orbital period, epoch of mid-eclipse, I-band magnitude and an approximate $V-I$ color outside eclipse, the depth of eclipse, number of transits observed (N_{tr}), and remarks. OII acronym in the remarks column indicates that the object was observed in the OGLE-II phase. For these stars both – the mean I-band magnitude and $V-I$ color from OGLE-II photometric maps were used to set the zero point of photometry, and both values are accurate to better than 0.05 mag. In the remaining cases the accuracy of the magnitude scale and $V-I$ color is not better than 0.1 mag.

Light curves in the graphical form are presented in Appendix: full phased light curve and close up around the eclipse. Additionally we also print there a finding chart – 60×60 arcsec subframe of the I-band template image centered on the star. North is up and East to the left in these images. For single transit stars, only the light curve around the transit and finding chart are presented.

6. Discussion

Results of our 2001 planetary and low-luminosity object transit campaign clearly indicate that the OGLE project reached photometric accuracy of millimagnitudes while observing millions of stars in the most crowded fields of the Galactic disk and bulge. Transit events with the depth as small as 10–20 millimagnitude can routinely be detected in the data collected by the OGLE-III hardware and processed by the OGLE-III software data pipeline. This opens up a new discovery channel of low-luminosity companions by photometric monitoring of millions of stars. We note that with the spectroscopic follow-up observations it will soon be possible to determine all basic parameters of these faint objects: planets, brown dwarfs or low-luminosity end of the main sequence stars.

A limited analysis is possible even now, without spectroscopic data. We estimate sizes of our transiting objects by modeling their light curves assuming a completely dark companion and using formulae provided by Sackett (1999). These were numerically integrated at the appropriate phase points to produce model light curves.

We found a possible solution for each candidate with the known period by analyzing the χ^2 of the model fit $\{R_s/a,\ R_c/R_s,\ i\}$ to the observational data, where a is semiaxis of the orbit, R_s – radius of the primary star, R_c – radius of the low luminosity companion and i – inclination of the orbit. In all cases we assumed the limb darkening coefficient $u=0.5$ (Al-Naimiy 1978).

T a b l e 2

OGLE-III planetary and low luminosity object transits

Name	RA (J2000)	DEC (J2000)	P [days]	T_0 −2452000	I [mag]	$V-I$ [mag]	ΔI [mag]	$N_{\rm tr}$	Rem.
OGLE-TR-1	$17^{h}51^{m}10^{s}.02$	$-30^{\circ}16'46''.2$	1.6009	61.14367	15.657	1.30	0.043	4	
OGLE-TR-2	$17^{h}51^{m}24^{s}.24$	$-30^{\circ}14'05''.9$	2.8131	61.86463	14.177	0.85	0.019	5	
OGLE-TR-3	$17^{h}51^{m}48^{s}.95$	$-30^{\circ}13'25''.1$	1.1899	60.22765	15.567	1.00	0.019	10	
OGLE-TR-4	$17^{h}51^{m}14^{s}.55$	$-30^{\circ}03'28''.3$	2.6188	60.21812	14.715	1.40	0.065	5	
OGLE-TR-5	$17^{h}51^{m}49^{s}.39$	$-30^{\circ}01'44''.3$	0.8082	60.47118	14.883	0.90	0.043	8	
OGLE-TR-6	$17^{h}51^{m}03^{s}.07$	$-29^{\circ}55'49''.8$	4.5487	61.05651	15.356	1.70	0.053	4	
OGLE-TR-7	$17^{h}52^{m}08^{s}.63$	$-29^{\circ}56'12''.7$	2.7179	61.42566	14.800	1.10	0.034	5	OII
OGLE-TR-8	$17^{h}52^{m}18^{s}.57$	$-29^{\circ}56'24''.6$	2.7152	61.01604	15.648	1.20	0.048	4	OII
OGLE-TR-9	$17^{h}51^{m}50^{s}.88$	$-29^{\circ}54'43''.4$	3.2687	61.42444	14.012	0.85	0.048	4	
OGLE-TR-10	$17^{h}51^{m}28^{s}.25$	$-29^{\circ}52'34''.9$	3.1037	60.88835	14.930	0.85	0.022	4	
OGLE-TR-11	$17^{h}50^{m}04^{s}.96$	$-29^{\circ}57'40''.7$	1.6154	60.37108	16.006	1.99	0.053	7	OII
OGLE-TR-12	$17^{h}50^{m}49^{s}.55$	$-30^{\circ}01'05''.6$	5.7721	61.53515	14.671	1.22	0.038	2	OII
OGLE-TR-13	$17^{h}50^{m}55^{s}.41$	$-30^{\circ}14'51''.2$	5.8534	64.68849	13.892	0.85	0.030	2	
OGLE-TR-14	$17^{h}54^{m}33^{s}.92$	$-30^{\circ}01'31''.5$	7.7978	62.28715	13.064	0.81	0.034	3	OII
OGLE-TR-15	$17^{h}54^{m}52^{s}.30$	$-29^{\circ}58'20''.4$	4.8746	61.18221	13.226	0.93	0.026	4	OII
OGLE-TR-16	$17^{h}54^{m}08^{s}.96$	$-29^{\circ}47'39''.3$	2.1386	60.33385	13.517	0.99	0.026	4	OII
OGLE-TR-17	$17^{h}54^{m}23^{s}.53$	$-29^{\circ}45'58''.4$	2.3171	62.35748	16.218	1.26	0.034	4	OII
OGLE-TR-18	$17^{h}54^{m}16^{s}.46$	$-29^{\circ}43'11''.9$	2.2280	61.07501	16.010	1.25	0.043	6	OII
OGLE-TR-19	$17^{h}54^{m}33^{s}.38$	$-29^{\circ}44'37''.8$	5.2821	61.89798	16.351	1.57	0.065	2	OII
OGLE-TR-20	$17^{h}53^{m}51^{s}.72$	$-29^{\circ}41'53''.8$	4.2835	63.87664	15.405	1.24	0.059	3	OII
OGLE-TR-21	$17^{h}54^{m}47^{s}.04$	$-29^{\circ}41'17''.4$	6.8925	66.11971	15.585	1.51	0.043	3	OII
OGLE-TR-22	$17^{h}54^{m}38^{s}.63$	$-29^{\circ}38'32''.0$	4.2750	61.48734	14.546	1.14	0.084	3	OII
OGLE-TR-23	$17^{h}54^{m}35^{s}.05$	$-29^{\circ}38'50''.7$	3.2866	61.79082	16.394	1.21	0.059	2	OII
OGLE-TR-24	$17^{h}53^{m}04^{s}.49$	$-29^{\circ}38'30''.2$	5.2821	63.80639	14.847	1.20	0.053	2	OII
OGLE-TR-25	$17^{h}52^{m}45^{s}.41$	$-29^{\circ}35'12''.1$	2.2181	62.13473	15.274	1.26	0.038	5	OII
OGLE-TR-26	$17^{h}53^{m}21^{s}.22$	$-29^{\circ}35'38''.8$	2.5389	61.49645	14.784	1.24	0.053	4	OII
OGLE-TR-27	$17^{h}53^{m}36^{s}.77$	$-29^{\circ}34'29''.5$	1.7149	61.13038	15.716	1.37	0.026	6	OII
OGLE-TR-28	$17^{h}52^{m}46^{s}.39$	$-29^{\circ}45'13''.9$	3.4051	63.10716	16.433	1.44	0.053	3	OII
OGLE-TR-29	$17^{h}52^{m}18^{s}.53$	$-29^{\circ}56'24''.7$	2.7159	61.01619	15.648	1.20	0.048	4	OII
OGLE-TR-30	$17^{h}52^{m}48^{s}.58$	$-30^{\circ}00'30''.1$	2.3650	61.92604	14.926	1.09	0.038	6	OII
OGLE-TR-31	$17^{h}53^{m}22^{s}.69$	$-29^{\circ}59'23''.1$	1.8832	60.79767	14.335	1.06	0.030	7	OII
OGLE-TR-32	$17^{h}56^{m}47^{s}.53$	$-29^{\circ}42'42''.0$	1.3433	60.35064	14.853	0.95	0.034	7	
OGLE-TR-33	$17^{h}56^{m}41^{s}.19$	$-29^{\circ}40'05''.3$	1.9533	60.54289	13.711	0.95	0.034	2	
OGLE-TR-34	$17^{h}56^{m}44^{s}.90$	$-29^{\circ}40'34''.5$	8.5810	62.74970	15.995	1.45	0.048	3	
OGLE-TR-35	$17^{h}57^{m}16^{s}.01$	$-29^{\circ}35'30''.5$	1.2599	60.98942	13.267	0.80	0.030	7	
OGLE-TR-36	$17^{h}57^{m}38^{s}.02$	$-29^{\circ}35'17''.2$	6.2516	62.37694	15.767	1.45	0.059	2	
OGLE-TR-37	$17^{h}57^{m}30^{s}.11$	$-29^{\circ}28'43''.6$	5.7197	60.57910	15.184	1.40	0.030	2	
OGLE-TR-38	$17^{h}56^{m}21^{s}.17$	$-29^{\circ}24'00''.4$	4.1015	62.50097	14.674	0.60	0.048	3	
OGLE-TR-39	$17^{h}57^{m}05^{s}.70$	$-29^{\circ}22'48''.7$	0.8152	60.81057	14.685	1.30	0.030	11	
OGLE-TR-40	$17^{h}57^{m}10^{s}.27$	$-29^{\circ}15'38''.1$	3.4318	60.03089	14.947	1.25	0.026	3	
OGLE-TR-41	$17^{h}55^{m}16^{s}.39$	$-29^{\circ}31'32''.1$	4.5170	62.29677	13.488	0.65	0.022	2	OII
OGLE-TR-42	$17^{h}55^{m}29^{s}.76$	$-29^{\circ}33'30''.8$	4.1610	63.67328	15.397	1.37	0.038	4	OII
OGLE-TR-43	$17^{h}51^{m}27^{s}.04$	$-29^{\circ}52'21''.8$	–	–	15.506	0.95	0.035	1	
OGLE-TR-44	$17^{h}50^{m}45^{s}.98$	$-30^{\circ}03'40''.1$	–	–	14.573	1.10	0.059	1	OII
OGLE-TR-45	$17^{h}50^{m}48^{s}.10$	$-30^{\circ}00'38''.7$	–	–	16.073	1.28	0.062	1	OII
OGLE-TR-46	$17^{h}54^{m}00^{s}.88$	$-29^{\circ}43'45''.7$	–	–	13.449	0.93	0.049	1	OII

As expected, many fits of similar quality can be obtained for an entire class of parameters. This corresponds to the fact that very similar shape of the eclipse can be obtained by a small companion with orbital inclination $i = 90°$ or larger one with smaller i transiting on the disk of larger star. However, the ratio of radii remains almost constant. Thus, if the stellar radius were known, the size of the companion and the inclination angle i could be derived unambiguously. The semiaxis of the orbit can be calculated from the determined orbital period, assuming that the stellar mass $M_s = 1$ $M_\odot$. The colors of our transit stars indicate that these stars have spectral types similar to, or later than the Sun.

The smallest size of the star and its companion is obtained when the transit is central, *i.e.*, for the inclination $i = 90°$. Non-central passage (smaller i) requires a larger size of both, the star and its companion. Table 3 lists the minimum size of the transiting companion and the corresponding size of the star to provide a feeling about the expected size of the observed objects. It should be remembered that semiaxis of the orbit scales as $M^{1/3}$, and therefore the same scaling is appropriate for the sizes of stars and companions listed in Table 3. In the close-up windows in the Appendix we show model light curves for central transit ($i = 90°$) drawn with a continuous bold line.

Table 3

Dimensions of stars and companions for central passage ($M_s = 1$ $M_\odot$)

Name	R_s [$R_\odot$]	R_c [$R_\odot$]	Name	R_s [$R_\odot$]	R_c [$R_\odot$]
OGLE-TR-1	0.99	0.18	OGLE-TR-22	1.68	0.42
OGLE-TR-2	1.75	0.21	OGLE-TR-23	0.99	0.21
OGLE-TR-3	1.48	0.18	OGLE-TR-24	1.45	0.29
OGLE-TR-4	1.60	0.35	OGLE-TR-25	1.43	0.24
OGLE-TR-5	1.01	0.18	OGLE-TR-26	1.15	0.23
OGLE-TR-6	1.65	0.33	OGLE-TR-27	1.88	0.26
OGLE-TR-7	1.37	0.22	OGLE-TR-28	1.76	0.35
OGLE-TR-8	0.85	0.16	OGLE-TR-29	0.87	0.17
OGLE-TR-9	1.36	0.26	OGLE-TR-30	1.38	0.23
OGLE-TR-10	0.84	0.11	OGLE-TR-31	1.60	0.24
OGLE-TR-11	1.03	0.21	OGLE-TR-32	0.88	0.14
OGLE-TR-12	0.89	0.15	OGLE-TR-33	1.26	0.20
OGLE-TR-13	1.49	0.22	OGLE-TR-34	1.92	0.36
OGLE-TR-14	2.02	0.32	OGLE-TR-35	1.12	0.17
OGLE-TR-15	3.02	0.42	OGLE-TR-36	1.46	0.31
OGLE-TR-16	2.49	0.35	OGLE-TR-37	2.24	0.34
OGLE-TR-17	1.53	0.25	OGLE-TR-38	0.95	0.18
OGLE-TR-18	1.09	0.20	OGLE-TR-39	0.97	0.14
OGLE-TR-19	0.84	0.18	OGLE-TR-40	0.73	0.10
OGLE-TR-20	1.16	0.24	OGLE-TR-41	1.55	0.20
OGLE-TR-21	2.38	0.43	OGLE-TR-42	1.55	0.26

Table 3 indicates that the companions cover a large range of sizes of low-luminosity objects. Many of them are certainly faint M-type stars. In several cases (*e.g.*, OGLE-TR-5, OGLE-TR-16), the light curves exhibit an ellipsoidal variation, indicating that the primary is tidally distorted, *i.e.*, the companion mass is not very small. There are eight objects (OGLE-TR-8, OGLE-TR-10, OGLE-TR-12, OGLE-TR-29, OGLE-TR-32, OGLE-TR-35, OGLE-TR-39, OGLE-TR-40) with companion radii of the order of 1.5 R_{Jup} or less, which implies that they may by planets, or brown dwarfs or low-luminosity stars. Note that the radius of the "hot Jupiter" orbiting and transiting HD 209458 is about 1.4 R_{Jup}.

The most intriguing and exciting objects within this group are certainly OGLE-TR-40 and OGLE-TR-10. Three and four individual transits, respectively, were observed in these stars, so the orbital periods are sound. The radius estimates of the companions as given in Table 3, 1.0 R_{Jup} and 1.1 R_{Jup}, respectively, are the smallest among our systems. Even if the transits were significantly non-central the radii of these objects would be smaller than 1.5 R_{Jup}. These objects appear to be most similar to the "hot Jupiter" companion to HD 209458.

The spectroscopic follow-up will provide a simple and very important clarification. The radial velocity amplitude will provide an estimate of the companion mass accurate enough to determine its nature: a planet, a brown dwarf, or a low mass star. The spectrum of the primary will provide an estimate of its mass and luminosity, and a refinement of the companion mass. Finally, a very accurate future photometry may refine system parameters even more.

Note, that a detection of a brown dwarf companion on a short period orbit would be at least as interesting as a detection of Jupiter mass planet. There appears to be a "brown dwarf desert", with very few objects in the mass range $10\ M_{Jup} - 100\ M_{Jup}$ (*cf.* Tabachnik and Tremaine 2001, and references therein). The spectroscopic follow-up of our 42 objects will either support or contradict the concept of the "desert".

There is a major problem with the mass – radius relation for lower main sequence stars, with the observed radii being 10–20% larger than model predictions (Torres and Ribas 2001, O'Brien, Bond and Sion 2001). There is a plausible explanation in terms of long living huge star spots (Spruit 1982, Spruit and Weiss 1986), but there are too few accurate radius determinations for a verification of that theory. The sample of eclipsing systems with lower main sequence secondaries will increase substantially as soon as the OGLE-III data will be searched for deeper eclipses than those presented in this paper.

In addition to 42 stars for which multiple transits were observed, we found four objects with low luminosity companions, but only one transit event detected in our data set. The lack of additional transits during our 2001 campaign indicates that the orbital periods of these objects are likely to be long.

The successful 2001 campaign proves that photometric detection of low-luminosity transiting objects is not only feasible but that transits can be routinely detected. Therefore it will be worthwhile to repeat similar observational campaigns in other directions of the Galactic disk. Such campaigns are planned in the coming seasons during the OGLE-III phase of our project.

The photometric data of OGLE-III transit objects presented in this paper are available in the electronic form from the OGLE archive:

http://www.astrouw.edu.pl/˜ogle
ftp://ftp.astrouw.edu.pl/ogle/ogle3/transits

or its US mirror

http://bulge.princeton.edu/˜ogle
ftp://bulge.princeton.edu/ogle/ogle3/transits

Acknowledgements. The paper was partly supported by the Polish KBN grant 2P03D01418 to M. Kubiak. Partial support to the OGLE project was provided with the NSF grant AST-9820314 to B. Paczyński. We acknowledge usage of The Digitized Sky Survey which was produced at the Space Telescope Science Institute based on photographic data obtained using The UK Schmidt Telescope, operated by the Royal Observatory Edinburgh.

REFERENCES

Alard, C., and Lupton, R. 1998, *Astrophys. J.*, **503**, 325.
Alard, C. 2000, *Astron. Astrophys. Suppl. Ser.*, **144**, 363.
Al-Naimiy, H.M. 1978, *Astr. Sp. Sc.*, **53**, 181.
Brown, T.M., and Charbonneau, D. 2000, in: "Disks, Planetesimals and Planets", *ASP Conference Series*, Vol. **219**, 584.
Brown, T.M., Charbonneau, D., Gilliland, R.L., Noyes, R.W., and Burrows, A. 2001, *Astrophys. J.*, **552**, 699.
Charbonneau, D., Brown, T.M., Latham, D.W., and Mayor, M. 2000, *Astrophys. J. Letters*, **529**, L45.
Deleuil, M., Barge, P., Defay, C., Léger, A., Rouan, D., and Schneider, J. 2000, in: "Disks, Planetesimals and Planets", *ASP Conference Series*, Vol. **219**, 656.
Gilliland, R.L., *et al.* 2000, *Astrophys. J. Letters*, **545**, L47.
Henry, G.W., Marcy, G.W., Butler, R.P., and Vogt, S.S. 2000, *Astrophys. J. Letters*, **529**, L41.
Marcy, G.W., and Butler, R.P. 1996, *Astrophys. J. Letters*, **464**, L147.
Mayor, M., and Queloz, D. 1995, *Nature*, **378**, 355.
Mazeh, T., and Zucker, S. 2002, astro-ph/0201337.
Mochejska, B.J., Stanek, K.Z., Sasselov, D.D., and Szentgyorgyi, A.H. 2002, astro-ph/0201244.
O'Brien, M.S., Bond, H.E., and Sion, E.M. 2001, *Astrophys. J.*, **563**, 971.
Quirrenbach, A., Cooke, J., Mitchell, D., and Safizadeh, N. 2000, in: "Disks, Planetesimals and Planets", *ASP Conference Series*, Vol. **219**, 566.
Sackett, P.D. 1999, in: "Planets Outside the Solar System: Theory and Observations," Eds. J.-M. Mariotti and D. Alloin, NATO-ASI Series, Kluwer, 189.
Spruit, H.C. 1982, *Astron. Astrophys.*, **108**, 348.
Spruit, H.C., and Weiss, A. 1986, *Astron. Astrophys.*, **166**, 167.
Street, R.A., *et al.* 2000, in: "Disks, Planetesimals and Planets", *ASP Conference Series*, Vol. **219**, 572.
Szymański, M. and Udalski, A. 1993, *Acta Astron.*, **43**, 91.
Tabachnik, S., and Tremaine, S. 2001, astro-ph/0107482.
Torres, G., and Ribas, I. 2002, astro-ph/0111167.
Udalski, A., Szymański, M., Kałużny, J., Kubiak, M., and Mateo, M. 1992, *Acta Astron.*, **42**, 253.

Udalski, A., Szymański, M., Kałużny, J., Kubiak, M., Krzemiński, W., Mateo, M., Preston, G.W., and Paczyński, B. 1993, *Acta Astron.*, **43**, 289.

Udalski, A., Kubiak, M., and Szymański, M. 1997, *Acta Astron.*, **47**, 319.

Udalski, A., Szymański, M., Kubiak, M., Pietrzyński, G., Woźniak, P., and Żebruń, K. 1998, *Acta Astron.*, **48**, 147.

Udalski, A., Soszyński, I., Szymański, M., Kubiak, M., Pietrzyński, G., Woźniak, P., and Żebruń, K. 1999, *Acta Astron.*, **49**, 223.

Udalski, A., Szymański, M., Kubiak, M., Pietrzyński, G., Soszyński, I., Woźniak, P., and Żebruń, K. 2000, *Acta Astron.*, **50**, 307.

Wolszczan,A., and Frail, D.A. 1992, *Nature*, **355**, 145.

Woźniak, P.R. 2000, *Acta Astron.*, **50**, 421.

Woźniak, P.R., Udalski, A., Szymański, M., Kubiak, M., Pietrzyński, G., Soszyński, I., and Żebruń, K. 2001, *Acta Astron.*, **51**, 175.

Woźniak, P.R., Udalski, A., Szymański, M., Kubiak, M., Pietrzyński, G., Soszyński, I., and Żebruń, K. 2001, *Acta Astron.*, **51**, in press, astro-ph/0201377.

Żebruń, K., Soszyński, I., Woźniak, P.R., Udalski, A., Kubiak, M., Szymański, M., Pietrzyński, G., Szewczyk, O., and Wyrzykowski, Ł. 2001, *Acta Astron.*, **51**, 317.